CSF infusion of TrkB agonist, 7,8-dihydroxyflavone, is ineffective in promoting remyelination in cuprizone and EAE models of multiple sclerosis

List title: 7,8-dihyroxyflavone in preclinical MS mouse models

Authors: Jessica L Fletcher[1,2*], Rhiannon J Wood[1] , Alexa R Prawdiuk[1], Ryan O'Rafferty[1], Ophelia Ehrlich[1], David G Gonsalvez[1,3], and Simon S Murray[1*]

[1]Department of Anatomy & Physiology, School of Biomedical Sciences, Faculty of Medicine, Dentistry & Health Sciences, University of Melbourne, VIC, Australia

[2]Menzies Institute for Medical Research, University of Tasmania, Hobart, TAS, Australia.

[3]Department of Anatomy and Developmental Biology, School of Biomedical Sciences, Monash University, VIC, Australia

***Corresponding author(s):**
Email: jessica.fletcher@utas.edu.au (JLF), Email: ssmurray@unimelb.edu.au (SSM)

Abstract

Small molecular weight functional mimetics of brain-derived neurotrophic factor (BDNF) which act via the TrkB receptor have been developed to overcome the pharmacokinetic limitations of BDNF as a therapeutic for neurological disease. Activation of TrkB on oligodendrocytes has been identified as a potential strategy for myelin repair in demyelinating conditions. Here, we tested the efficacy of intracerebroventricular infusion of TrkB agonist 7,8-dihydroxyflavone (DHF) to promote myelin repair in the cuprizone model and alter the course of experimental autoimmune encephalomyelitis (EAE). In these two distinct mouse models used for the preclinical testing of remyelinating therapeutics, we found that DHF infusion increased the percentage of myelin basic protein and density of oligodendrocyte progenitor cells (OPCs) in the corpus callosum of female C57BL/6 mice after cuprizone demyelination. However, DHF did not alter the percentage of axons myelinated or increase the density of post-mitotic oligodendrocytes in this model. Direct cerebrospinal fluid infusion of DHF also had no effect on the clinical course of EAE, and examination of the lumbar spinal cord after 21 days of treatment revealed extensive demyelination. These results indicate that direct cerebrospinal fluid infusion of DHF is ineffective at promoting myelin repair in toxin-induced and inflammatory models of demyelination.

Keywords: TrkB, oligodendroglia, multiple sclerosis, experimental autoimmune encephalomyelitis, cuprizone

33 **Introduction**

34 Neurotrophins have long been identified as therapeutic candidates to treat neurologic disorders due to
35 their ability to promote neuronal survival and differentiation as well as synaptic plasticity [1]. However, it
36 is only comparatively recently that the effects neurotrophins mediate *via* glial cells have received
37 attention as a potential mechanism to prevent neurodegeneration [2,3]. This includes the effect of brain-
38 derived neurotrophic factor (BDNF), which has been shown to promote central nervous system (CNS)
39 myelination via its TrkB receptor [4,5]. That BDNF elicits oligodendroglial differentiation and myelination
40 by activating TrkB is highly relevant for the auto-immune demyelinating disease, multiple sclerosis (MS).
41 Although there are now many immune-targeted therapies that can significantly modify the course of
42 relapsing-remitting MS, there are no treatments which can prevent or reverse the axon loss and neuron
43 death that lead to the increasing severity of neurologic dysfunction experienced by patients with
44 progressive MS [6,7]. Therefore, neuroprotective therapeutic strategies that can also promote myelin
45 repair—such as selectively targeting the TrkB receptor—are highly sought-after as adjunct treatments to
46 the immuno-modulatory therapies clinically available for MS.

47

48 Although attractive as a remyelinating therapeutic, BDNF itself has poor pharmacokinetic properties – it
49 is a large molecule unable to cross the blood-brain barrier, that is rapidly cleared systemically [8] and is
50 non-selective, interacting with both TrkB and the pan-neurotrophin receptor $p75^{NTR}$ [1,2,9]. Collectively,
51 these properties of BDNF have led to the development of multiple smaller molecular weight TrkB agonists,
52 also called functional BDNF-mimetics [1,10–12]. This includes TDP6 and LM22A-4, both which promote
53 myelin repair in an oligodendroglial TrkB-dependent manner in the cuprizone model of de- and
54 remyelination, in which MS therapies for myelin repair are frequently tested [13,14]. Notably, 7,8-
55 dihydroxyflavone (DHF), the most widely used TrkB agonist within the biomedical literature (Fig. S1) has

56 not previously been tested in cuprizone. However, in experimental autoimmune encephalomyelitis (EAE)
57 it has been shown to significantly reduce the course of clinical signs when administered prophylactically
58 via intra-peritoneal injection [15]. In addition, DHF has undergone extensive biochemical and biophysical
59 characterisation to demonstrate its ability to interact with the extracellular domain of TrkB and elicit TrkB
60 phosphorylation *in vitro* [16]. As a flavonoid, DHF has also been shown to act as an anti-oxidant, promoting
61 survival in neuronal cell culture models of oxidative stress independent of TrkB receptor expression
62 [17,18]. Overall, the ability of DHF to elicit TrkB signalling and act as a neuroprotective anti-oxidant makes
63 it a promising candidate to promote myelin repair in the context of MS and inflammatory demyelination.

64

65 To test the capacity of DHF to promote myelin repair in response to inflammatory demyelination, two
66 mouse models of myelin loss were used, the cuprizone model and EAE. In the toxin-induced cuprizone
67 model, mature oligodendrocytes are selectively killed resulting in profound demyelination and
68 inflammatory gliosis, followed by rapid remyelination once cuprizone is withdrawn [13,14,19]. However,
69 cuprizone does not mimic the auto-immune attack against myelin which characterises MS. This is achieved
70 in EAE, in which mice are immunised against a myelin protein (typically myelin oligodendrocyte
71 glycoprotein, MOG), which results in neuroinflammation and clinical signs of ascending paralysis, but
72 determining if remyelination has occurred in EAE is challenging [20]. In the current study DHF was
73 administered directly to the CNS via intracerebroventricular infusion into the cerebrospinal fluid in both
74 models. This was done to enable comparison with previous cuprizone studies investigating the
75 remyelinating potential of TrkB activation [13,14], and to limit modulation of the peripheral immune
76 system in EAE. Additionally, in EAE, DHF was administered at the onset of clinical signs to reflect the likely
77 experience of people with MS, who would receive treatment following initial clinical presentation.

78

Results

7,8-dihydroxylfavone fails to enhance myelin repair in the cuprizone model of de- and remyelination

We have previously shown that 7-day ICV infusions of the structural peptide mimetic of BDNF, TDP6 and the partial TrkB agonist, LM22A-4 increase the level of MBP expression, the proportion of myelinated axons and myelin sheath thickness during remyelination after cuprizone-induced demyelination [13,14]. To determine if DHF could mediate the same effect as a TrkB agonist in the same context (Fig. 1A), we first assessed the level of MBP immunostaining in the caudal corpus callosum (Fig. 1C). This revealed 7-day infusion of DHF during remyelination resulted in an increased percentage area of MBP immunostaining compared to infusion with the aCSF vehicle ($p=0.012$), but not when compared to the 14% DMSO vehicle ($p=0.22$; Fig. 1B). To confirm whether this increase in MBP staining was due to a pro-myelinating effect, we next performed electron microscopy (EM; Fig. 1D), comparing the proportion of myelinated axons in the caudal corpus callosum of mice that received the aCSF vehicle, to those that received DHF, but did not detect a change ($p=0.23$, Fig. 1E). However, electron dense myelin debris was more frequently observed in the caudal callosum of mice that received DHF (Fig. 1D). Collectively, both the MBP and EM analyses indicate that 7-day ICV infusion of DHF itself does not enhance remyelination above either the infusion of aCSF or DMSO vehicle infusion.

7,8-dihydroxyflavone increases OPC density after cuprizone-induced demyelination

Infusion of either TDP6 or LM22A-4 for 7 days during remyelination increased the density of total Olig2$^+$ oligodendroglia in the caudal corpus callosum, primarily by increasing the density of Olig2$^+$CC1$^+$ post-mitotic oligodendrocytes [13,14]. Here, we sought to determine if DHF, mediated the same effect by performing cell counts on sagittal brain sections triple immunolabeled for Olig2 to identify all cells in the oligodendroglial lineage, PDGFRα to identify oligodendrocyte precursor cells (OPCs) and CC1 to identify

post-mitotic oligodendrocytes (Fig. 2A). This identified a trend towards an increased density of Olig2$^+$ oligodendroglia in the caudal corpus callosum of mice that received DHF treatment compared to those that received either aCSF or the DMSO vehicle (Fig. 2B). Treatment with DHF increased the density of OPCs (p=0.0002, Fig 2C), whereas DMSO infusion did not result in a detectable difference in OPC density in the caudal corpus callosum when compared to mice treated the aCSF vehicle (p=0.71, Fig. 2C). There was no detectable change (p=0.96) in the density of Olig2$^+$CC1$^+$ post-mitotic oligodendrocytes in the caudal corpus callosum of mice that received DHF, compared to those that received aCSF or DMSO (Fig 2D). These data indicate that ICV infusion of DHF, but not its DMSO vehicle during the remyelinating period selectively triggers OPC proliferation.

7,8-dihydroxyflavone administered directly into the CNS after onset of clinical signs does not alter the clinical course of EAE

Others have shown that daily intraperitoneal injection of DHF in DMSO from the day of EAE induction can improve its clinical course and improve neuropathological outcomes including the extent of inflammation and demyelination [15]. We sought to build on these findings to determine if DHF treatment had a direct effect on the CNS during EAE via ICV infusion, and if it could alter the course of EAE after the onset of clinical signs (Fig. 3A). We found that compared to the treatment with DMSO vehicle, ICV infusion of DHF from Day 13 when mice exhibited tail weakness and/or weakness of one hindlimb, did not alter the clinical course of EAE (Treatment: p=0.47, Fig. 3B). We also observed that male mice induced with EAE had a tended to have more severe phenotype than female mice (Interaction Sex × Day: p=0.052, data not shown) but were underpowered to determine if DHF treatment altered this. Consistent with no effect of DHF on clinical score, we also found that compared to sham EAE animals (Fig. 3C), there remained profound demyelination in the lumbar spinal cord of DHF-treated EAE at Day 35, using SCoRe and

125 Fluromyelin to detect compact myelin and myelin debris (Fig. 3C). Overall, these results indicate that
126 direct infusion of DHF into the CNS after the onset of clinical signs, is unable to alter the course of EAE.

127

128 **Discussion**

129 We sought to determine if direct infusion into the CNS of the TrkB agonist DHF, could promote myelin
130 repair in two animal models used preclinically to evaluate therapeutics for MS. We found that DHF failed
131 to promote myelin repair in the cuprizone model of de- and remyelination, with no increase in the
132 proportion of myelinated axons after cuprizone withdrawal compared to the aCSF treated vehicle. This
133 was despite increases in the percentage area of the caudal corpus callosum positive for MBP staining. DHF
134 also failed to alter the clinical course of EAE, an immune-driven model of demyelination, when it was
135 administered via ICV infusion after the initial onset of tail and/or hindlimb weakness. These results are
136 inconsistent with previous findings, wherein recombinant BDNF, and other compounds, TDP6 and LM22A-
137 4, shown to activate TrkB signalling in the cuprizone model, and in multiple *in vitro* contexts [12,14,21,22],
138 did promote remyelination by increasing the proportion of myelinated axons and/or density of post-
139 mitotic oligodendrocytes [13,14]. They also contrast findings in EAE, where intraperitoneal administration
140 of DHF improved the clinical course, preserved myelination and reduced neuroinflammation in the spinal
141 cord [15]. In the current study, the only indication that DHF may have pro-myelinating properties was a
142 significant increase in OPC density in the caudal corpus callosum at the end of 7 days of remyelination.

143

144 Proliferation of OPCs is required to replace the myelinating oligodendrocytes that are killed during
145 cuprizone induced demyelination. The increased OPC density in response to DHF infusion during the
146 remyelinating phase in cuprizone-demyelinated mice could be a priming event that precedes robust
147 myelin repair that extends past the 7-day treatment period examined here. ICV infusion of LM22A-4 also

148 significantly increased OPC density in the caudal corpus callosum after 7-days of infusion in cuprizone-
149 demyelinated mice [14]. However, the LM22A-4-mediated increase in OPC density was accompanied by
150 a strong pro-differentiation effect, typical of oligodendroglial TrkB signalling [23], with a significant
151 increase in post-mitotic oligodendrocytes and myelinated axons [14]. Promoting oligodendrocyte
152 differentiation and myelination of axons are two measures of effective myelin repair that DHF was unable
153 to elicit in a mouse model where endogenous remyelination commences within 3-days [13,14,24,25].
154 More importantly, these are capabilities that are absolutely essential for a candidate remyelinating
155 therapy for MS, in which the primary aim is to overcome arrested OPC differentiation [6,26].

156

157 The poor efficacy of DHF as a remyelinating therapeutic for MS when administered to the CNS was also
158 demonstrated in EAE as it did not modify the clinical course, and demyelination and neuroinflammation
159 remained extensive. Testing potential MS therapeutics in EAE is widely considered to be required due to
160 the complex interactions between the immune system and the CNS that occur in MS, and most disease-
161 modifying MS treatments clinically available are immuno-modulatory and have been tested in this model
162 [7]. Previously, DHF was shown to prevent EAE from progressing beyond tail weakness when administered
163 via intraperitoneal injection from the day of EAE induction [15]. This is in contrast with the strategy used
164 here, where DHF was administered directly to the CNS via ICV infusion and did not commence until EAE
165 mice demonstrated tail and/or hindlimb weakness. The timing of treatment from the onset of clinical signs
166 is more likely to represent what MS patients will experience.

167

168 The dose of DHF used here is 131x lower than the intraperitoneal delivered dose [15] and this may account
169 for the lack of efficacy in the current study. However, it is reflective of the same scaling used of effective
170 doses of LM22A-4 and TDP6 from *in vitro* [12,27] to *in vivo* application in the cuprizone model (13,14). It

171 is also possible that the ICV infusion of DHF into the cerebrospinal fluid failed to reach the lumbar and
172 sacral spinal cord which are severely affected by peripheral immune cell infiltration and demyelination
173 that precipitate the ascending paralysis characteristic of EAE. This seems highly likely based on the extent
174 of demyelination present in the lumbar spinal cord of DHF-treated EAE mice at Day 35. It would be
175 interesting to compare how high-dose peripheral delivery of DHF from clinical onset influences the clinical
176 course of EAE, and if this strategy would be as effective as the prophylactic regime previously tested [15].

177

178 Alternatively, it is possible that DHF mediates its effects in a TrkB-independent manner or with altered
179 timing that is not directly comparable to typical BDNF-TrkB signalling dynamics. Increased OPC density in
180 cuprizone remyelination and the reduced severity of EAE in the previous study [15] in response to DHF
181 treatment are not what would be expected based on the effect of TrkB activation on autoreactive T-cells
182 [28] or oligodendroglia [5,13,14,23]. TrkB activation on autoreactive T-cells has been reported to promote
183 their survival and propagate the autoimmune attack against myelin [28]. Instead, peripheral
184 administration of DHF from the day of MOG sensitisation exerted an anti-inflammatory effect with
185 significantly fewer CD45+ leukocytes, CD3+ T-cells, CD20+ B- cells and CD11b+ macrophages present in
186 the spinal cord of the peripherally DHF-treated EAE mice [15]. It is possible this response could been due
187 to the anti-oxidant properties of DHF [17,18,29] which are able to promote neuronal cell line survival in a
188 TrkB-independent manner[17,18]. Similarly, oligodendroglial TrkB activation is strongly associated with a
189 pro-differentiation effect mediated by MAPK-ERK1/2 signalling [5,30]. Interestingly, DHF has been
190 reported to be biased towards PI3K-Akt signalling [16,31] which is associated with promoting OPC survival
191 [32,33]. This could potentially explain the increase in OPCs. Further, DHF, like LM22A-4 and 6 other TrkB
192 agonists, have come under scrutiny for their inability to transduce TrkB signalling in a BDNF-like manner
193 [34]. Overall, the data from DHF-treated cuprizone mice, the previous study in EAE [15], and several other
194 studies examining the mode of action of DHF [16–18,29,34] suggest that DHF may not act in a manner

195 consistent with typical BDNF-TrkB signalling. This indicates that studies using DHF to mimic of BDNF
196 activation of TrkB to elucidate TrkB receptor function should be interpreted with this caveat in mind.

197 The lack of pro-myelinating effect of DHF after cuprizone induced demyelination and its failure to modify
198 the disease course of EAE when directly administered to the CNS suggest that DHF does not have the key
199 characteristics required to be a viable remyelinating therapeutic for demyelinating diseases. Further, the
200 results of the current study, combined with existing literature on DHF and its mode of action, suggest that
201 DHF may not always elicit its effects in a BDNF-like manner.

202 **Materials & Methods**

203 *Experimental animals*

204 Male and female C57BL/6 mice, aged 6-7-weeks old were purchased from the Animal Resource Centre
205 (Perth, Australia) and group housed in specific pathogen-free conditions at the Melbourne Brain Centre
206 Animal Facility, under a 12 hour light / dark cycle with *ad libitum* access to food and water. Animals were
207 habituated to the new housing environment for a minimum of 7 days. All procedures were performed
208 with approval from the Florey Institute of Mental Health and Neuroscience Animal Ethics Committee (#12-
209 042, #18-024) and followed the Australian Code of Practice for the Care and Use of Animals for Scientific
210 Purposes.

211 *Cuprizone-induced demyelination*

212 At 8 weeks of age, female mice were fed 0.2% cuprizone in normal chow (Teklad Custom Diets) for 6-
213 weeks to induce demyelination. Cuprizone was then removed, and mice were killed (*n*=2/cohort) or
214 underwent intracerebroventricular pump implantation to receive aCSF, DMSO vehicle or DHF for 7 days
215 as previously described. Only female mice were used in cuprizone experiments due to the increased
216 incidence of MS in females [35].

217

218 *Experimental autoimmune encephalomyelitis and clinical monitoring*

219 To induce experimental autoimmune encephalomyelitis (EAE), male and female mice, aged 8 weeks
220 received subcutaneous injections to both flanks and base of the tail of MOG_{35-55} peptide (125µg total,
221 Mimotopes) emulsified 1:1 (vol/vol) in Freund's complete adjuvant (BD Cat# 263810) containing
222 additional *Mycobacterium tuberculosis* (5mg/mL, BD Cat# 231141). A subset of mice received a sham
223 emulsion of 1:1 phosphate buffered saline (PBS) in Freund's complete adjuvant with 5mg/mL *M.*
224 *tuberculosis*. Injections of emulsion were followed by intraperitoneal injection of 400ng pertussis toxin
225 (List Biological Laboratories, Sapphire Biosciences Cat# 70323-44-3) in 0.1mL in sterile PBS. Mice were
226 anaesthetized for all injections on Day 0 with exposure to 4% isoflurane in air which was maintained for
227 less than 5 mins at 0.5-1.5% isoflurane through a nose cone. On Day 3, all mice received a second
228 intraperitoneal injection of 400ng pertussis toxin. Mice were weighed and assessed for EAE clinical signs
229 daily. EAE clinical scores was graded according to Table 1.

230 *Intracerebroventricular delivery of 7,8-dihydroxyflavone (DHF)*

231 Cuprizone and EAE mice received intracerebroventricular (ICV) osmotic minipumps (Azlet) vehicle as
232 previously described [13] of 762ng/day 7,8-dihydroxyflavone (equivalent to 250µM for the 7 day infusion
233 with 0.5µL/hr flowrate, or 500µM for the 21 day infusion with 0.25µL/hr flowrate, DHF), artificial aCSF
234 (cuprizone mice only) or 14% (v/v) DMSO. DHF doses were based on previous *in vitro* studies, wherein 250
235 to 500nM of DHF was required to reach the same level of neuronal survival as BDNF [11]. Briefly, mice
236 were anaesthetised with 2-4% isoflurane in normal air, scalp was shaved, and mice were fitted into a
237 stereotaxic frame receiving 1.5-2.5% isoflurane in air via a nose cone. A sagittal incision was made across
238 the midline of the scalp, and a 1.5mm burr hole was made at +0.5mm rostral and -0.7mm lateral from
239 Bregma using a microdrill. Reservoirs were placed subcutaneously along the flank and cannulae were
240 implanted and fixed in place using an ethyl cyanoacrylate adhesive (Loctite). Vicyrl sutures (Ethicon, Cat#
241 J492G) were used to close head wounds and animals placed in recovery chamber at 32°C and closely

242 monitored until ambulatory, before being single-housed in standard cages (Technoplast). Cuprizone
243 treated mice received 7-day pumps (Azlet #1007D) on the final day of cuprizone exposure before being
244 returned to normal chow and tolerated the procedure well. All ICV minipumps were implanted in
245 cuprizone treated animals on the same days as animals reported in (13, 14). EAE mice received 28-day
246 pumps (Azlet #2004) on Day 13 if they demonstrated tail weakness or tail paralysis. Of 19 EAE mice that
247 underwent the procedure 10 died due to anaesthetic complications or were excluded due to poor wound
248 healing. One EAE-induced mouse did not develop clinical signs by Day 13 and was excluded. Due to high
249 mortality and exclusion rate, ICV implantation in EAE mice was discontinued and available sample size is
250 limited.

251 *Tissue collection, processing, and immunofluorescence*

252 All mice were anaesthetised with isoflurane and euthanased with barbiturates (Lethabarb, Vibrac
253 Australia) before transcardial perfusion with sterile 0.1M PBS, then ice-cold 4% paraformaldehyde (PFA).
254 Brains from cuprizone mice and the lumbar enlargement of spinal cords from EAE mice were removed.
255 Tissues were post-fixed overnight in 4% PFA, then washed in 0.1M PBS and cryoprotected in 30% sucrose.
256 For electron microscopy (EM) studies of cuprizone mice, the first millimeter of the right hemisphere from
257 the sagittal midline was selected and placed in Kanovsky's buffer overnight and washed in 0.1M sodium
258 cacodylate before resin embedding at the Centre for Advanced Histology and Microscopy at the Peter
259 MacCallum Centre. Remaining cuprizone brain tissue was oriented sagittally, while EAE spinal cords were
260 oriented longitudinally for embedding in OCT (Tissue-tek) and frozen in isopentane over dry ice. Tissue
261 blocks were stored at -80°C until sectioning at 16µm (brain) or 20µm (spinal cord) using a cryostat
262 maintained at -16 to -17°C, with sections collected on Superfrost^{+} slides. Slides were air-dried and stored
263 at -80°C before use. Approximately 70-100 µm separated adjacent sections on the same slide and sagittal
264 brain sections cut beyond ± 2.64mm from the lateral midline were excluded as previously [13,14].

265 Primary antibodies for immunostaining are listed in Table 2. Slides were immersed in three exchanges of
266 0.1M PBS, before overnight incubation at room temperature with primary antibodies diluted in 10%
267 normal donkey serum (NDS) with 0.3% Triton-X 100 in 0.1M PBS. Next, slides were washed three times in
268 0.1M PBS before incubation with appropriate AlexaFluor-conjugated secondary antibodies
269 (ThermoFisher) for 2 hours at room temperature, after which slides underwent a final wash and were
270 cover slipped using aqueous mounting solution (Dako). After air-drying slides were stored at 4°C until
271 imaging. Modifications for MBP staining included immersing slides in ice-cold 100% methanol for 10mins
272 prior first wash. When used, Hoeschst33342 (ThermoFisher) was the nuclear counterstain.

273 *Fluorescence imaging and analysis*

274 All imaging was performed blinded to treatment group. For sagittal sections, imaging was restricted to
275 the caudal region of the corpus callosum approximately -1.1mm to -3.0mm from Bregma, and tracts
276 contributing to the dorsal hippocampal commissure were excluded as previously [13]. Spinal cord sections
277 were from approximately L2 to S1, with imaging restricted to the lateral white matter tracts. For each
278 analysis, a minimum of three sections per animal were imaged.

279 MBP staining was imaged under a 20x (0.8 NA) lens using an RGB camera (AxioVision Hr, Zeiss) attached
280 to an epifluorescence Axioplan2 Imager (Zeiss) microscope using consistent exposure times. All remaining
281 stains were imaged using Zeiss LSM510 Meta, LSM780 or LSM880 confocal microscope with 405nm,
282 488nm, 561nm or 633nm laser lines. Images acquired on the LMS780 and 880 were processed (tiles
283 stitched, and maximum z-projections produced) using Zen Black software. Uniform acquisition settings
284 were used for each staining batch. Brightness and contrast were adjusted if needed for counting and
285 presentation purposes.

286 Oligodendroglial cell counts were performed manually as described in [14] using FIIJ/Image J and
287 expressed as number of cells/mm^2.

288 *Electron microscopy and analysis*

289 Electron microscopy and analysis was performed as described in [13]. Briefly, after region selection on
290 semi-thin sections collected on glass slides and stained with 1% toluidine blue, ultrathin sections were
291 collected on 3mm x 3mm copper grids and examined using a JEOL 1011 transmission electron microscope,
292 and imaged using a MegaView III CCD cooled camera operated with iTEM AnalySIS software (Olympus
293 Soft Imaging Systems). A minimum of six distinct fields of view were captured at 10 000x magnification
294 per animal, and used to count myelinated axons in FIJI/Image J. For this analysis, DHF treated animals
295 were compared to animals that solely received aCSF vehicle treated animals previously published in
296 [13,14] as DMSO treated animals were not processed for EM analyses. Sectioning, post-staining and EM
297 imaging were all performed at the Centre for Advanced Histology and Microscopy, Peter MacCallum
298 Centre.

299 *Spectral confocal reflectance (SCoRe) microscopy*

300 SCoRe microscopy on longitudinally oriented spinal cord from EAE mice was performed as described in
301 [36], and combined with fluoromyelin (ThermoFisher Cat# F34652, RRID: AB_2572213) and Iba1
302 immunostaining. Briefly, before imaging sections were washed in 0.1M PBS and incubated at 4°C with
303 goat-anti Iba1 (Table 2) in 10% NDS without 100% Triton-X 100 to keep myelin membranes intact for 2
304 nights in a humified chamber. Sections were washed and incubated with donkey anti-goat AlexaFluor488
305 for 4 hours at room temperature, before being washed and then incubated in 50% fluoromyelin in PBS for
306 20 min, and washed thoroughly, before being mounted with #1.5 coverslips (Zeiss, 1.5H, 170±5µm). SCoRe
307 images were captured using a Zeiss LSM880 confocal microscope using 40x oil immersion lens (1.3 NA)
308 and immersion oil (Zeiss, Immersol 518F), with a refractive index of 1.518. Closely, matched refractive
309 index of the coverslip and immersion oil prevented reflection of light from the glass coverslip interfering
310 with SCoRe signal. Lasers with 488nm, 561nm and 633nm wavelengths were passed through acousto-

311 optical tunable filters (AOTF) 488-640 filter/splitter and a 20/80 partially reflective mirror. Reflected light
312 was collected using three photodetectors set to collect light through narrow bands defined by prism and
313 mirror slides, centred around the laser wavelengths.

314 *Experimental design and statistical analyses*

315 All quantitative assessments were performed by an observer blinded to animal and treatment identity
316 with a minimum of 3 animals per group assessed. All EAE clinical score assessments were performed by
317 observers blinded to treatment group. Statistical testing including 1-way ANOVA and student's unpaired
318 t-tests were performed in GraphPad Prism (v.8). Restriction maximum likelihood (REML) mixed models
319 were performed in jamovi [37] using GAMLj (v.2.0.6) to evaluate the effect of treatment and day post-
320 induction on clinical score [38]. A p-value less than 0.05 was considered significant. Mean ± standard
321 deviation (SD) plotted in all graphs.

322 **References**

323 1. Longo, F. M. & Massa, S. M. Small-molecule modulation of neurotrophin receptors: a strategy for
324 the treatment of neurological disease. *Nat Rev Drug Discov* **12,** 507–525 (2013).

325 2. Fletcher, J. L. *et al.* Brain-Derived Neurotrophic Factor in Central Nervous System Myelination: A
326 New Mechanism to Promote Myelin Plasticity and Repair. *Int. J. Mol. Sci.* **19,** 4131 (2018).

327 3. Fulmer, C. G. *et al.* Astrocyte-Derived BDNF Supports Myelin Protein Synthesis after Cuprizone-
328 Induced Demyelination. *J. Neurosci.* **34,** 8186–8196 (2014).

329 4. Wong, A. W., Xiao, J., Kemper, D., Kilpatrick, T. J. & Murray, S. S. Oligodendroglial expression of
330 TrkB independently regulates myelination and progenitor cell proliferation. *J. Neurosci.* **33,** 4947–
331 57 (2013).

332 5. Van't Veer, A. *et al.* Brain-derived neurotrophic factor effects on oligodendrocyte progenitors of

333 the basal forebrain are mediated through TrkB and the MAP kinase pathway. *J. Neurosci. Res.* **87,**
334 69–78 (2009).

335 6. Murphy, N. A. & Franklin, R. J. M. *Recruitment of endogenous CNS stem cells for regeneration in*
336 *demyelinating disease*. *Funct. Neural Transplant. IV Transl. to Clin. Appl. Part B* **231,** (Elsevier
337 B.V.).

338 7. Faissner, S., Plemel, J. R., Gold, R. & Yong, V. W. Progressive multiple sclerosis: from
339 pathophysiology to therapeutic strategies. *Nat. Rev. Drug Discov.* **18,** 905–922 (2019).

340 8. Poduslo, J. F. & Curran, G. L. Permeability at the blood-brain and blood-nerve barriers of the
341 neurotrophic factors: NGF, CNTF, NT-3, BDNF. *Mol. Brain Res.* **36,** 280–286 (1996).

342 9. Chao, M. V. Neurotrophins and their receptors: a convergence point for many signalling
343 pathways. *Nat. Rev. Neurosci.* **4,** 299–309 (2003).

344 10. O'Leary, P. D. & Hughes, R. A. Design of potent peptide mimetics of brain-derived neurotrophic
345 factor. *J. Biol. Chem.* **278,** 25738–25744 (2003).

346 11. Jang, S.-W. *et al.* A selective TrkB agonist with potent neurotrophic activities by 7,8-
347 dihydroxyflavone. *Proc. Natl. Acad. Sci. U. S. A.* **107,** 2687–92 (2010).

348 12. Massa, S. M. *et al.* Small molecule BDNF mimetics activate TrkB signaling and prevent neuronal
349 degeneration in rodents. *J. Clin. Invest.* **120,** 1774–1785 (2010).

350 13. Fletcher, J. L. *et al.* Targeting TrkB with a Brain-Derived Neurotrophic Factor Mimetic Promotes
351 Myelin Repair in the Brain. **38,** 7088–7099 (2018).

352 14. Nguyen, H. T. H. *et al.* TrkB Agonist LM22A-4 Increases Oligodendroglial Populations During
353 Myelin Repair in the Corpus Callosum. *Front. Mol. Neurosci.* **12,** 205 (2019).

354 15. Makar, T. K. *et al.* TrkB agonist, 7,8-dihydroxyflavone, reduces the clinical and pathological
355 severity of a murine model of multiple sclerosis. *J. Neuroimmunol.* **292,** 9–20 (2016).

356 16. Liu, X. *et al.* Biochemical and Biophysical Investigation of the Brain-derived Neurotrophic Factor
357 Mimetic 7,8-Dihydroxyflavone in the Binding and Activation of the TrkB Receptor. *J. Biol. Chem.*
358 **289,** 27571–27584 (2014).

359 17. Han, X. *et al.* Antioxidant action of 7,8-dihydroxyflavone protects PC12 cells against 6-
360 hydroxydopamine-induced cytotoxicity. *Neurochem. Int.* **64,** 18–23 (2014).

361 18. Chen, J. *et al.* Antioxidant activity of 7,8-dihydroxyflavone provides neuroprotection against
362 glutamate-induced toxicity. *Neurosci. Lett.* **499,** 181–185 (2011).

363 19. Skripuletz, T., Gudi, V., Hackstette, D. & Stangel, M. De- and remyelination in the CNS white and
364 grey matter induced by cuprizone: The old, the new, and the unexpected. *Histol. Histopathol.* **26,**
365 1585–1597 (2011).

366 20. Baker, D., Gerritsen, W., Rundle, J. & Amor, S. Critical appraisal of animal models of multiple
367 sclerosis. **17,** 647–657 (2011).

368 21. Schmid, D. A. *et al.* A TrkB small molecule partial agonist rescues TrkB phosphorylation deficits
369 and improves respiratory function in a mouse model of Rett syndrome. *J. Neurosci.* **32,** 1803–10
370 (2012).

371 22. Wong, A. W. *et al.* TDP6, a brain-derived neurotrophic factor-based trkB peptide mimetic,
372 promotes oligodendrocyte myelination. *Mol. Cell. Neurosci.* **63,** 132–140 (2014).

373 23. Huang, Y. *et al.* Tropomyosin Receptor Kinase B Expressed in Oligodendrocyte Lineage Cells
374 Functions to Promote Myelin Following a Demyelinating Lesion. *ASN Neuro* **12,** (2020).

375 24. Fernández-Castañeda, A. *et al.* The active contribution of OPCs to neuroinflammation is mediated
376 by LRP1. *Acta Neuropathol.* **139,** 365–382 (2020).

377 25. Geraghty, A. C. *et al.* Loss of Adaptive Myelination Contributes to Methotrexate Chemotherapy-
378 Related Cognitive Impairment. *Neuron* **103,** 250-265.e8 (2019).

379 26. Chang, A., Tourtellotte, W. W., Rudick, R. & Trapp, B. D. Premyelinating Oligodendrocytes in
380 Chronic Lesions of Multiple Sclerosis. *N. Engl. J. Med.* **346,** 165–173 (2002).

381 27. Wong, A. W. *et al.* TDP6, a brain-derived neurotrophic factor-based trkB peptide mimetic,
382 promotes oligodendrocyte myelination. *Mol Cell Neurosci* **63,** 132–140 (2014).

383 28. De Santi, L., Annunziata, P., Sessa, E. & Bramanti, P. Brain-derived neurotrophic factor and TrkB
384 receptor in experimental autoimmune encephalomyelitis and multiple sclerosis. *J. Neurol. Sci.*
385 **287,** 17–26 (2009).

386 29. Cho, S. J. *et al.* 7,8-dihydroxyflavone protects high glucose-damaged neuronal cells against
387 oxidative stress. *Biomol. Ther.* **27,** 85–91 (2019).

388 30. Du, Y., Lercher, L. D., Zhou, R. & Dreyfus, C. F. Mitogen-activated protein kinase pathway
389 mediates effects of brain-derived neurotrophic factor on differentiation of basal forebrain
390 oligodendrocytes. *J. Neurosci. Res.* **84,** 1692–1702 (2006).

391 31. Wu, C.-H. *et al.* Post-Injury Treatment with 7,8-Dihydroxyflavone, a TrkB Receptor Agonist,
392 Protects against Experimental Traumatic Brain Injury via PI3K/Akt Signaling. *PLoS One* **9,** e113397
393 (2014).

394 32. Ebner, S., Dunbar, M. & McKinnon, R. D. Distinct roles for PI3K in proliferation and survival of
395 oligodendrocyte progenitor cells. *J. Neurosci. Res.* **62,** 336–345 (2000).

396 33. Ness, J. K., Mitchell, N. E. & Wood, T. L. IGF-I and NT-3 Signaling Pathways in Developing
397 Oligodendrocytes: Differential Regulation and Activation of Receptors and the Downstream
398 Effector Akt. *Dev. Neurosci.* **24,** 437–445 (2002).

399 34. Boltaev, U. *et al.* Multiplex quantitative assays indicate a need for re-evaluating reported small-
400 molecule TrkB agonists. **10,** 1670 (2017).

401 35. Wallin, M. T. *et al.* The prevalence of MS in the United States. *Neurology* **92,** e1029–e1040
402 (2019).

403 36. Gonsalvez, D. G. *et al.* Imaging and Quantification of Myelin Integrity After Injury With Spectral
404 Confocal Reflectance Microscopy. *Front. Mol. Neurosci.* **12,** 275 (2019).

405 37. Project, T. jamovi. jamovi (v. 1.2). at (2020)

406 38. Gallucci, M. GAMLj: General, Mixed and Generalized Models module for Jamovi. at (2020)

407 39. Guyenet, S. J. *et al.* A simple composite phenotype scoring system for evaluating mouse models
408 of cerebellar ataxia. *J. Vis. Exp.* (2010). doi:10.3791/1787

409

410 **Acknowledgements**

411 We thank Dr Chris Dwyer and Michele Binder (Florey Institute for Neuroscience and Mental Health) for
412 their assistance with the EAE model. We acknowledge the staff and facilities of the Biological Optical
413 Microscopy Platform (University of Melbourne), Centre for Advanced Histology and Microscopy (Peter
414 MacCallum Centre) and Florey Advanced Microscopy and Immunohistochemistry Service. JLF was
415 supported by a MS Research Australia Postdoctoral Fellowship (#14-056). This work was funded by an
416 Australian National Health and Medical Research Council Project Grant (#APP1105108) awarded to SSM.

This work was supported by the Assistant Secretary of Defense for Health Affairs, endorsed by the Department of Defense, USA, through the Multiple Sclerosis Research Program W81XWH-17-MSRP-IIRA under award no. MS170031 to Simon Murray. Opinions, interpretations, conclusions, and recommendations are those of the authors and not necessarily endorsed by the Assistant Secretary of Defense for Health Affairs or Department of Defense (USA).

Author contributions

JLF: conceptualization, data curation, formal analysis, investigation, project administration, supervision, visualization, writing – original draft preparation, writing – review & editing. RJW: investigation, methodology, project administration, validation, writing – revieW & editing. ARP, RO & OE: investigation. DGG: methodology, resources, validation, writing – review & editing. SSM: conceptualization, funding acquisition, project administration, resources, supervision, writing – review & editing.

Data Availability Statement

Data will be made available upon request to the corresponding authors.

Competing Interests Statement

The authors declare they have no competing interests.

Figure Legends

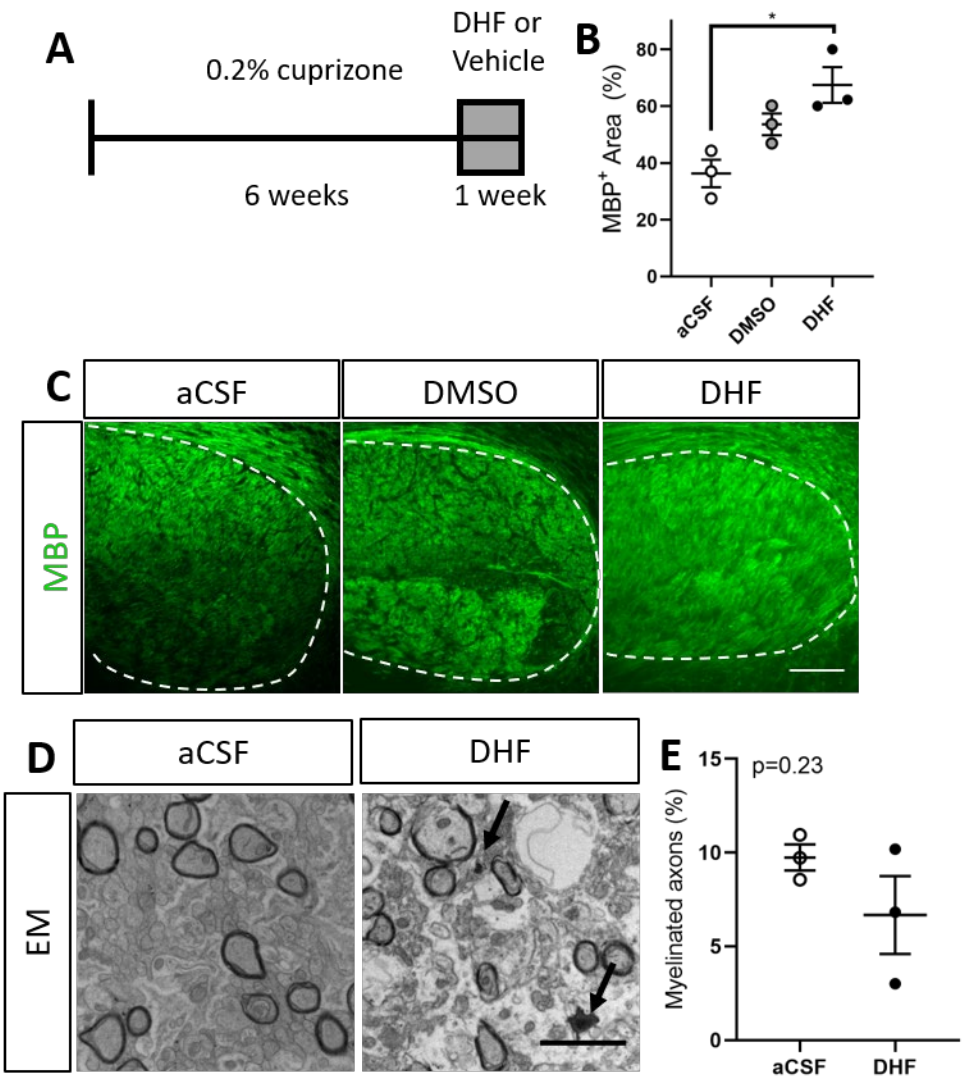

433

434 **Figure 1: 7,8-dihydroxylfavone increases area of myelin basic protein (MBP) immunostaining but does**

435 **not increase the percentage of myelinated axons during remyelination.** (a) Schematic of experimental

436 paradigm, where cuprizone demyelinated mice received either DHF, aCSF or 14% DMSO vehicle *via* ICV

437 infusion for 1 week. (b) Animals receiving DHF had an increased percentage area MBP^+ immunostaining

438 in the cadual corpus callosum, compared to mice that received the aCSF vehicle (p=0.012) but not

439 compared to those that received the DMSO vehicle (p=0.22) (n=3/group, 1-way ANOVA, $F_{2,6}$=0.09,

440 Tukey's post-hoc comparison). Representative (c) micrographs of MBP immunostaining (scale bar =

441 100µm) and (d) electron micrographs (scale bar = 2µm) in the caudal corpus callosum of aCSF, DMSO

442 and DHF treated animals (arrows: myelin debris). (E) DHF treatment did not alter the percentage of

443 axons myelinated in the caudal corpus callosum during remyelination, compared to animals that

444 received aCSF (n=3/group, unpaired t-test, $F_{2,2}$=9.04).

445

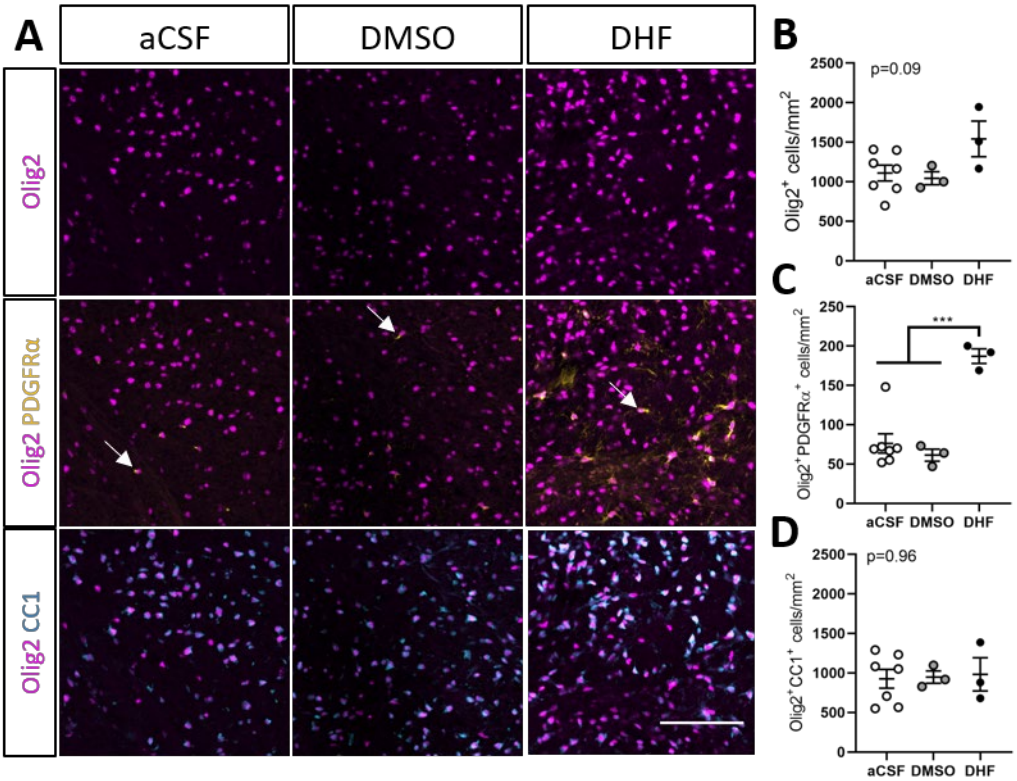

446

447 **Figure 2: Increased oligodendrocyte progenitor cell density in the caudal corpus callosum of mice**

448 **treated with 7,8-dihydroxylfavone during remyelination.** (a) Representative micrographs for Olig2-

449 PDGFRα-CC1 triple immunolabelling in the cadual corpus callosum of mice treated with aCSF, DMSO or

450 DHF during remyelination. Scale bar=100µm. Brightness and contrast have been adjusted to improve

451 visibility. (b) The density of Olig2+ oligodendroglia demonstrated a trend increase in mice that were

452 treated with DHF compared to those that received the aCSF and DMSO vehicles. This was driven by (c)

453 an increase (p=0.0002) in Olig2+PDGFRα+ OPC (arrows in A) densities in the corpus callosum of mice

454 that received DHF compared to those that received aCSF or DMSO vehicles. (d) There was no change in

455 the density of Olig2+CC1+ cells in the corpus callosum of mice treated with DHF compared to aCSF and

456 DMSO. For (b-c) (*n*=3-7/group, 1-way ANOVA, Tukey's post-hoc comparison).

457

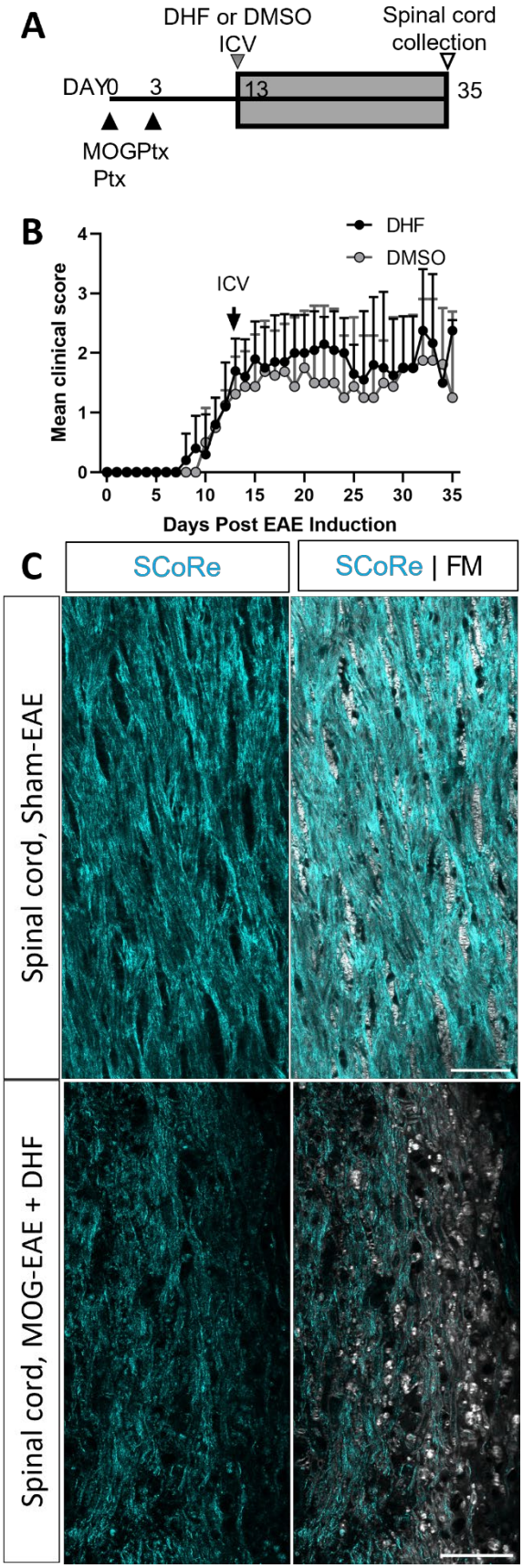
A
DHF or DMSO
ICV
Spinal cord
collection
DAY0
3
13
35
MOGPtx
Ptx
B
DHF
DMSO
ICV
Mean clinical score
Days Post EAE Induction
C
SCoRe
SCoRe | FM
Spinal cord, Sham-EAE
Spinal cord, MOG-EAE + DHF

458

459 **Figure 3: Direct CSF infusion of 7,8-dihydroxyflavone after the onset of clinical signs does not alter the**
460 **disease course or restore myelin in EAE.** (a) Schematic of experimental paradigm of EAE experiments,
461 where ICV infusion into the CNS of either DHF or the DMSO vehicle commenced on Day 13 after the
462 onset of tail weakness. (b) There was no change (p=0.46) in the mean clinical score of mice that received
463 either DHF or DMSO (n=4-5/group, mean ± SD plotted). (c) Longitudinal section of the lateral white
464 matter of the lumbar spinal cord of a sham-EAE mouse at Day 35, showing intact compact myelin as
465 detected by SCoRe imaging (cyan) and fluromyelin staining (white), as compared to spinal cord from a
466 MOG-EAE mouse at Day 35 that received DHF, where there remained prevalent myelin debris. Scale bar
467 = 50µm.

468 **Tables**

469 **Table 1: Scoring criteria for daily assessment of clinical signs in EAE mice.**

Score	Description
0	Normal appearance, tail lifts and normal gait.
1	Normal gait, but tail is weak and is slow or fails to curl around finger when stroked.
1.5	Tail is weak, is slow / fails to curl around finger when stroked. Normal appearing gait, but some hindlimb weakness when performing hindlimb clasp test [39].
2.0	Complete tail paralysis, can no longer be lifted by mouse and fails to curl around finger when stroked.
2.25	Complete tail paralysis and some hindlimb weakness when performing hindlimb clasp test.
2.5	Complete tail paralysis and hindlimb weakness when performing hindlimb clasp test.
2.75	Complete tail paralysis and paralysis of one hindlimb when walking.
3.0	Complete tail and hindlimb paralysis, but maintains righting reflex, when placed on back / side.
3.5	Complete tail and hindlimb paralysis, with forelimb weakness and loss of righting reflex or signs of urinary / faecal incontinence. Requires immediate euthanasia.
4.0	Spontaneous death.

470

471 **Table 2: Antibodies used for immunostaining**

Antibody	Maker for	Manufacturer	RRID	Concentration Used
Monoclonal rat anti-MBP	Myelin basic protein	Millipore (MAB386)	AB_9497	1:200
Polyclonal rabbit anti-Olig2	Oligodendrocyte lineage	Millipore (AB9610)	AB_570666	1:200
Polyclonal goat anti-PDGFRα	Oligodendrocyte progenitor cell	R&D Systems (AF1062)	AB_2236897	1:200
Monoclonal mouse anti-CC1	Post-mitotic oligodendrocyte	Millipore (OP-80)	AB_2057371	1:200
Polyclonal goat anti-Iba1	Macrophages/microglia	Abcam (ab5076)	AB_22244	1:200

472

473

474 **Supplementary Figure**

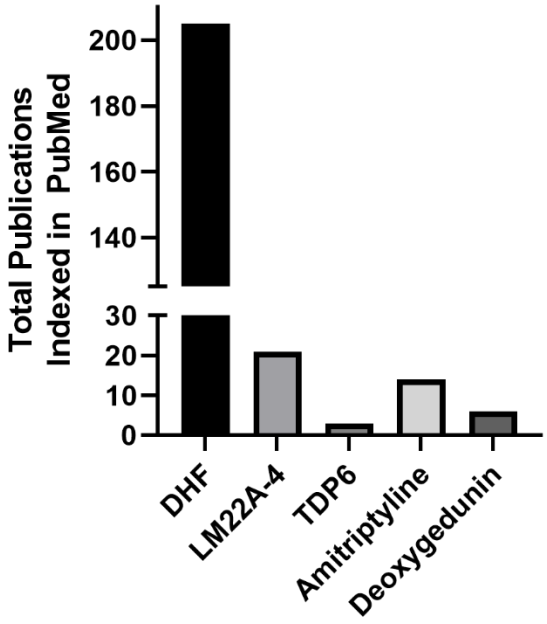

475

476 **Fig. S1: Total number of publications for each TrkB agonist indexed in PubMed**. Each TrkB agonist was
477 used as a search term in PubMed and the 'results by year' were downloaded and summed. Note for DHF
478 and Amitriptyline TrkB was included as an additional search term and only publications since their
479 characterisation as partial TrkB agonists were used (ie. from 2010 for DHF and 2007 for amitriptyline).
480 Search date: 7 October 2022